Inorganica Chimica Acta, 155 (1989) 113–123

Binding of Oxysulfur Anions to Macrocyclic Iron(II,III): $[(Fe(TPP))_2SO_4]$ and $[Fe(Me_6[14]\text{-}4,11\text{-}dieneN_4)(S_2O_5)]$

MARTHA S. REYNOLDS and R. H. HOLM*

Department of Chemistry, Harvard University, Cambridge, MA 02138, U.S.A.

(Received June 1, 1988)

Abstract

In an attempt to produce substrate–Fe(II) complexes potentially relevant to the mechanism of action of sulfite reductase, several anaerobic reaction systems were investigated. The system Fe(TPP) + SO_2 in benzene afforded $[(Fe(TPP))_2SO_4]$ (**1**), which was obtained in single crystal form as the solvate $[(Fe(TPP))_2SO_4]\cdot C_6H_6\cdot 2SO_2$. This compound crystallizes in orthorhombic space group $P2_122_1$ with a = 12.647(2), b = 13.483(3), c = 23.409(6) Å and Z = 2. Complex **1** contains five-coordinate Fe(III) units bridged by sulfate ion binding as a monodentate ligand to each metal. The structure of **1** is closely similar to that in a differently solvated, rhombohedral lattice reported earlier. The oxidized product results from traces of dioxygen and is probably formed from a bridged peroxide intermediate in a reaction demonstrated earlier. The system $[Fe(Me_6[14]\text{-}4,11\text{-}dieneN_4)(MeCN)_2]^{2+}$ + $(n\text{-}Bu_4N)HSO_3$ in acetonitrile yielded yellow, high-spin $[Fe(Me_6[14]\text{-}4,11\text{-}dieneN_4)(S_2O_5)]$ (**2**). Compound **2** crystallizes as the acetonitrile monosolvate in monoclinic space group $C2/c$ with a = 9.575(3), b = 16.557(4), c = 15.409(4) Å, β = 96.85(2)° and Z = 4. Complex **2** contains a chelating disulfite, generated in the equilibrium $2HSO_3^- \rightleftharpoons S_2O_5^{2-} + H_2O$. Dimensions of coordinated and free disulfite are not significantly different; however, the ligand is disordered around a C_2 axis passing through the Fe atom and bisecting the S–S bond of the chelate ring. This is the first structure of a transition metal disulfite complex. The results suggest the conditions necessary to the formation of an authentic sulfite or bisulfite complex of a Fe(II) tetraaza macrocycle, species potentially suitable as models of the enzyme–substrate complex of sulfite reductase.

Introduction

The sulfur cycle is the means by which inorganic sulfur is incorporated in the biosphere [1, 2]. Biological utilization requires reduction of oxidized sulfur to the oxidation level of sulfide. Assimilatory and dissimilatory sulfite reductases, found in fungi, algae and green plants, are responsible for part of this process by catalyzing the reduction of sulfite to sulfide in the six-electron process of reaction (1). Reduced sulfur then reacts with *O*-acetylserine on the biosynthetic pathway to cysteine. Similarly, reduced nitrogen is obtained by enzymatic reduction of nitrite to ammonia in another six-electron process. Sulfite and nitrite reductases appear to have in common a unique active-site catalytic assembly: a siroheme, the site of substrate binding when in the Fe(II) state [3], coupled structurally and electronically to a Fe_4S_4 cluster [4] via a cysteinate sulfur bridge [5].

$$SO_3^{2-} + 6H^+ + 6e^- \longrightarrow S^{2-} + 3H_2O \quad (1)$$

An ultimate understanding of multielectron reductions requires identification of intermediates and those factors which stabilize and activate them for subsequent steps in the overall reduction process. In the case of assimilatory enzymes, these factors are manipulated such that no intermediate levels of substrate reduction are detected during catalysis. It is, therefore, of interest to prepare and examine the reduction of Fe(II) complexes containing oxysulfur or sulfur substrates as terminal ligands, ranging in sulfur oxidation state from 4+ to 2–. Pathways (2) and (3) illustrate potential substrate oxidation states differing by two electrons. The three highest oxidation states in the latter scheme are derived from those in the former by removal of a water molecule. Several of the species have alternative formulations, e.g. Fe–S as Fe^{IV}=S.

$$Fe\text{–}SO_3^{2-} \longrightarrow Fe\text{–}SO_2^{2-} \longrightarrow Fe\text{–}SO \longrightarrow Fe\text{–}S^{2-} \quad (2)$$

$$Fe\text{–}SO_2 \longrightarrow Fe\text{–}SO \longrightarrow Fe\text{–}S \longrightarrow Fe\text{–}SH_2 \quad (3)$$

Examples of well-defined complexes with terminal sulfur ligands of varying oxidation state are known. Confining attention to the iron vertical group, $[Ru(NH_3)_4(HSO_3)_2]$ [6], $[Ru(NH_3)_5SO_2]Cl_2$ [7], Na_5-

*Author to whom correspondence should be addressed.

0020-1693/89/$3.50

$[Fe(CN)_5(SO_3)]\cdot xH_2O$ [8, 9] and $K[(C_5H_5)Fe(CO)_2SO_2]$ [10] have been prepared by simple ligand substitution or addition reactions and contain metal(2+) and S(4+). The two SO_2 complexes are part of an extensive set of such complexes with transition metals [11]. Coordinated sulfur(2+) in the form of $[M(P\text{-}i\text{-}Pr_3)_2(SO)Cl]$ (M = Rh, Ir) [12] and $[Rh(SO)X(PPh_3)]_2$ (X = Cl, Br) [13] has been obtained by the *in situ* generation of sulfur monoxide from thiirane S-oxide and stilbene episulfoxide, respectively. No iron-group complexes containing S(2+) are known, nor are any with S(0) or S(2−) as in Fe^{IV}=S. However, the S(2−) complexes $[Fe^{III}(TAP)SH]$ [14] (TAP = *meso*-tetra(*p*-methoxyphenyl)porphyrinate(2−)) and $[Ru(NH_3)_5SH_2](BF_4)_2$ [15] have been prepared. These results, while fragmentary, suggest that at least some of the species in pathways (2) and (3) may be accessible.

In the present work, iron complexes of porphyrins, Schiff bases and tetraaza macrocycles were considered. As representatives of the most oxidized form of substrate, bisulfite (HSO_3^-) and sulfur dioxide were examined as ligands. Two sulfur–oxygen complexes of iron were structurally characterized. One is a new crystalline form of the sulfate-bridged dimer of (*meso*-tetraphenylporphinato)iron(III), $[(Fe(TPP))_2SO_4]$ (**1**) [16, 17]. The other is $[Fe(Me_6[14]\text{-}4,11\text{-}dieneN_4)(S_2O_5)]$ (**2**), a bidentate disulfite complex of Fe(II) in the Curtis-type macrocycle $Me_6[14]\text{-}4,11\text{-}dieneN_4$ (**3**). This is the first structurally defined transition metal disulfite complex.

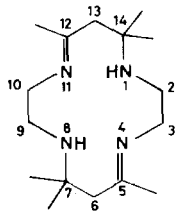

3

Experimental

Preparation of Compounds

meso-Tetraphenylporphine [18] and Fe(TPP)Cl [19] were prepared as described. $[Fe(TPP)]_2O$ was obtained by washing a dichloromethane solution of Fe(TPP)Cl with aqueous base [20]; the product was purified by column chromatography using neutral alumina (grade I). Fe(TPP) was prepared by the reduction of $[Fe(TPP)]_2O$ with ethanethiol in benzene [21]. The complex $[Fe(Me_6[14]\text{-}4,11\text{-}dieneN_4)(MeCN)_2](CF_3SO_3)_2$ [22] and $(n\text{-}Bu_4N)HSO_3$ [23] were synthesized by published methods. All other reagents and solvents were of commercial grade and were dried and purified as appropriate. All reactions and manipulations were carried out under a pure dinitrogen atmosphere.

[(Fe(TPP))$_2$SO$_4$] (1)

In a typical preparation, SO_2 was bubbled through a solution containing 40 mg of Fe(TPP) in 30 ml of benzene for 2 h. The solution volume was reduced *in vacuo* and degassed hexanes were layered on top of the solution. Deep purple crystals formed overnight at room temperature. The absorption spectrum (λ_{max} (C_6H_6) 410, 507, 571, 646, 683 nm) and ^1H NMR spectrum (δ (C_6D_6) 70.4 (8), 12.4 (*m*-H), 10.6 (*m*-H′), 6.6 (*p*-H)) are essentially identical to those reported by Phillippi *et al.* [16] for $[(Fe(TPP))_2SO_4]$, prepared by reaction of $[Fe(TPP)]_2O$ with 1 equivalent of 6 M H_2SO_4.

Disulfito(5,7,7,12,14,14-hexamethyl-1,4,8,11-tetraazacyclotetradeca-4,11-diene)iron(II), [Fe(Me$_6$[14]-4,11-diene-N$_4$)(S$_2$O$_5$)] (2)

$[Fe(Me_6[14]\text{-}4,11\text{-}dieneN_4)(MeCN)_2](CF_3SO_3)_2$ (2.00 g, 2.80 mmol) was dissolved in 100 ml of freshly distilled and degassed acetonitrile to give a red solution. Addition of 1.80 g (5.60 mmol) of $(n\text{-}Bu_4N)HSO_3$ caused an immediate color change to pale orange. The solution volume was reduced by one half *in vacuo* and a pale yellow powder precipitated. Recrystallization from acetonitrile afforded 0.44 g (32%) of product as a yellow crystalline solid, which was found by ^1H NMR and crystallography to be an acetonitrile monosolvate. The compound was dried prior to analysis. *Anal.* Calc. for $C_{16}H_{32}FeN_4O_5S_2$ (desolvated form): C, 40.00; H, 6.71; Fe, 11.62; N, 11.66; S, 13.35. Found: C, 39.40; H, 6.35; Fe, 11.54; N, 11.48; S, 13.10%. Absorption spectrum (MeCN): λ_{max} (ϵ_M) 252 (3490), 350 (597), 858 (9), 1080 (7) nm. ^1H NMR ($Me_2SO\text{-}d_6$, 22 °C): δ 103.4 (CH_2), 58.9 (CH_2), 32.8 (CH_2), 28.1 (CH_3), 25.2 (CH_2), 12.6 (CH_3), 0.75 (CH_3), −0.74 (CH_2), −47.8 (CH_2); ($CDCl_3$, 22 °C): δ 98.8 (CH_2), 40.2 ($2CH_2$), 25.9 (CH_3), 14.8 (CH_3), 5.73 (CH_2), −3.81 (CH_3), −7.26 (CH_2), −66.3 (CH_2). μ_{eff} = 5.07 μ_B ($CDCl_3$, 23 °C).

Crystallographic Studies

[(Fe(TPP))$_2$SO$_4$]·C$_6$H$_6$·2SO$_2$

Single crystals of compound **1** were obtained by vapor diffusion of pentane into a SO_2-saturated benzene solution of the complex at room temperature over a two-week period. The deep purple crystals were collected, washed with pentane, dried briefly, and stored under dinitrogen. A suitable crystal was mounted under dinitrogen in a glass capillary using Apiezon grease, and the capillary was flame-sealed. Diffraction experiments were performed at ambient temperature on a Nicolet P3F diffractometer using Mo Kα radiation and a graphite monochromator.

TABLE 1. Summary of Crystal Data, Intensity Collections and Refinement Parameters for $[(Fe(TPP))_2(SO_4)]\cdot C_6H_6\cdot 2SO_2$ (1) and $[Fe(Me_6[14]\text{-}4,11\text{-dieneN}_4)(S_2O_5)]\cdot MeCN$ (2)

	1	2
Formula	$C_{94}H_{62}Fe_2N_8O_8S_3$	$C_{18}H_{35}FeN_5O_5S_2$
Molecular weight	1639.47	521.78
a (Å)	12.647(2)	9.575(3)
b (Å)	13.483(3)	16.557(4)
c (Å)	23.409(6)	15.409(4)
β (°)		96.85(2)
Crystal system	orthorhombic	monoclinic
V (Å^3)	3992(1)	2425(1)
Z	2	4
$d_{calc.}$ (g/cm^3)	1.31	1.37
Space group	$P2_122_1$ (no. 18)	$C2/c$ (no. 15)
Crystal size (mm)	0.6 × 0.5 × 0.2	0.4 × 0.3 × 0.1
Absorption coefficient μ (cm^{-1})	4.70	7.7
Scan type	ω scan	ω scan
Scan speed (°/min)	2.0–29.0	2.0–29.0
Scan width (°)	0.4 below $K\alpha_1$ to 0.4 above $K\alpha_2$	0.4 below $K\alpha_1$ to 0.4 above $K\alpha_2$
Background/scan time ratio	0.25	0.25
Data collection limits	$3° \leq 2\theta \leq 55°$ $(+h, +k, +l)$	$3° \leq 2\theta \leq 55°$ $(+h, +k, \pm l)$
Total data collected	5498	5522
No. unique intensity	5294	2440
No. with $F_o > n\sigma(F)$	3707, $n = 4$	1050, $n = 6$
No. parameters	521	148
Weighting factor, g [a]	0.035941	0.024410
Final difference map (e$^-$/Å^3)	<0.66	<1.42
$R(F)$[b]	0.0681	0.0980
$R_w(F)$[a, c]	0.0758	0.0952
Goodness of fit	0.5438	0.78
Max shift/e.s.d. for last cycle	0.04	0.000

[a]The weighting scheme for least-squares refinement is $w = 1/(\sigma^2(F_o) + |g||F_o|^2)$. [b]$R(F) = \Sigma||F_o| - |F_c||/\Sigma|F_o|$. [c]$R_w(F) = \Sigma(w^{1/2}||F_o| - |F_c||)/\Sigma(w^{1/2}|F_o|)$.

Data collection parameters are summarized in Table 1. The final orientation matrix and unit cell parameters were obtained from 25 machine-centered reflections with $20° \leq 2\theta \leq 25°$. Intensities of three standard reflections examined every 123 reflections showed no significant decay over the course of data collection. The data were corrected for Lorentz and polarization effects and an empirical absorption correction was applied by using the programs XTAPE and XEMP, respectively, of the SHELXTL program package (Nicolet XRD Corporation, Madison, WI, USA). Axial photographs indicated Laue class *mmm*. The systematic absences *h00* ($h = 2n + 1$) and *00l* ($l = 2n + 1$) uniquely determine the space group as $P2_122_1$ (no. 18); successful solution and refinement of the structure confirmed this choice of space group. Atom scattering factors were taken from a standard source [24]. The SHELXTL and SHELXTL-PLUS program packages were employed for the structure solution and refinement. The structure was solved using a combination of direct methods and Fourier techniques. Isotropic refinement converged at 13.8%. Some, but not all, hydrogen atoms were located in the difference Fourier maps. In the final stages of refinement, therefore, all hydrogen atoms were placed at fixed distances of 0.96 Å with thermal parameters set to 1.2X the isotropic temperature factor of the bound carbon atom. Full-matrix least-squares refinement was performed with anisotropic thermal parameters on all non-hydrogen atoms. Inversion of coordinates gave slightly higher residual parameters, indicating that the initially chosen enantiomer was correct. Positional parameters are listed in Table 2. Drawings were produced by using the program XP in the SHELXTL-PLUS program package.

[Fe(Me$_6$[14]-4,11-dieneN$_4$)(S$_2$O$_5$)]·MeCN

Single crystals of compound 2 as pale yellow blocks were obtained by recrystallization from acetonitrile at −20 °C. To prevent desolvation, a crystal of appropriate size was coated with epoxy before insertion into a glass capillary, which was then flame-sealed. Data collection was performed as for 1;

TABLE 2. Positional Parameters ($\times 10^4$) for $[(Fe(TPP))_2\text{-}SO_4]\cdot C_6H_6\cdot 2SO_2$ (1)

Atom[a]	x/a	y/b	z/c
Fe	5686.2(8)[b]	3718.8(7)	6256.0(4)
S(1)	5000	3167(2)	7500
O(1)	5295(5)	3894(4)	7022(2)
O(2)	4020(13)	2706(12)	7321(6)
N(1)	4265(5)	3979(4)	5839(2)
N(2)	5408(5)	2218(5)	6121(3)
N(3)	7284(5)	3368(5)	6305(3)
N(4)	6140(5)	5116(5)	5992(3)
C(a1)	3829(7)	4915(6)	5740(3)
C(a2)	3460(6)	3323(6)	5742(3)
C(a3)	4455(6)	1794(6)	5990(4)
C(a4)	6058(7)	1468(6)	6321(4)
C(a5)	7659(6)	2474(6)	6465(4)
C(a6)	8138(7)	4020(6)	6298(4)
C(a7)	7141(6)	5527(6)	6028(3)
C(a8)	5472(6)	5891(6)	5868(3)
C(b1)	2734(6)	4812(6)	5599(4)
C(b2)	2511(7)	3841(7)	5591(4)
C(b3)	4513(8)	752(6)	6077(4)
C(b4)	5493(7)	548(6)	6304(5)
C(b5)	8792(7)	2518(8)	6573(5)
C(b6)	9070(7)	3486(8)	6462(5)
C(b7)	7108(6)	6568(6)	5919(4)
C(b8)	6067(8)	6781(6)	5814(4)
C(m1)	3533(8)	2287(6)	5806(4)
C(m2)	7096(7)	1581(6)	6494(4)
C(m3)	8079(6)	5018(6)	6172(3)
C(m4)	4379(7)	5813(5)	5762(3)
C(1)	2586(7)	1674(7)	5662(5)
C(2)	2418(10)	1392(8)	5110(6)
C(3)	1491(15)	861(9)	4968(8)
C(4)	773(13)	732(11)	5382(14)
C(5)	968(11)	926(16)	5914(12)
C(6)	1880(11)	1426(13)	6084(9)
C(7)	7656(7)	648(7)	6698(5)
C(8)	8139(10)	191(9)	5919(8)
C(9)	8664(12)	−854(11)	6504(11)
C(10)	8723(15)	−1007(12)	7080(14)
C(11)	8235(22)	−385(14)	7465(14)
C(12)	7697(15)	476(13)	7303(8)
C(13)	9084(6)	5612(7)	6183(4)
C(14)	9468(7)	5990(9)	5313(4)
C(15)	10341(10)	6616(11)	5670(6)
C(16)	10848(8)	6837(8)	6160(7)
C(17)	10480(10)	6462(10)	6666(7)
C(18)	9572(8)	5851(9)	6692(5)
C(19)	3806(7)	6771(6)	5678(4)
C(20)	3349(9)	7021(7)	5153(4)
C(21)	2827(11)	7924(8)	5091(5)
C(22)	2769(9)	8589(7)	5532(5)
C(23)	3223(7)	8339(7)	6048(4)
C(24)	3732(7)	7436(6)	6115(4)
C(25)	0	1603(16)	5000
C(26)	814(17)	2045(20)	2680(7)
C(27)	863(21)	3000(23)	2677(8)
C(28)	0	3564(12)	2500

(continued)

TABLE 2. *(continued)*

Atom[a]	x/a	y/b	z/c
S(2)	12494(4)	4148(6)	7050(2)
O(3)	11603(12)	3518(18)	7007(9)
O(4)	12358(18)	4954(16)	7360(9)

[a]The atom labeling scheme for the porphyrin ring is provided in Fig. 1; that for the benzene and sulfur dioxide molecules of solvation is given below.

[b]e.s.d.s in least significant figures are given in parentheses in this and succeeding Tables.

parameters for collection and structure refinement are given in Table 1. Axial photographs indicated Laue group $2/m$. The systematic absences hkl ($h + k = 2n + 1$), $h0l$ ($h, l = 2n + 1$), $0kl$ ($k = 2n + 1$), $hk0$ ($h + k = 2n + 1$), $0k0$ ($k = 2n + 1$), $h00$ ($h = 2n + 1$), and $00l$ ($l = 2n + 1$) are consistent with space groups Cc and $C2/c$. Simple E statistics calculated by MULTAN did not conclusively indicate centrosymmetry of the lattice. The assumed molecular geometry was thought to preclude the requisite two-fold axis or inversion center for $Z = 4$ in $C2/c$. However, attempted solution and refinement in the acentric space group led to poor convergence. Consequently, the centrosymmetric space group was assumed [25], and the crystallographically imposed two-fold axis through the Fe atom was accommodated by modeling disorder of the $S_2O_5^{2-}$ ligand as $O_{2.5}S\text{–}SO_{2.5}$, a composite of $O_2S\text{–}SO_3$ and $O_3S\text{–}SO_2$. The structure was solved as for **1**. Convergence of the model during least-squares refinement (SHELXTL-PLUS) confirmed the choice of the centrosymmetric space group. Full-matrix least-squares refinement was completed with anisotropic thermal parameters on all non-hydrogen atoms. Hydrogen atoms were placed as for **1**. Positional parameters are collected in Table 3.

Other Physical Measurements

Absorption spectra were measured on a Cary 219 or Varian 2300 spectrophotometer. ^1H NMR spectra were recorded on a Bruker WM-300, AM-300, or AM-250 spectrometer. Deuterated solvents were degassed prior to use and stored in a dry box. Magnetic susceptibility determinations were made by the Evans method [26], modified for superconducting spectrometers [27], in deuteriochloroform with t-butylmethylether as a reference. Solvent susceptibilities [28] and diamagnetic corrections [29] were taken from tabulated values.

TABLE 3. Positional Parameters ($\times 10^4$) for [Fe(Me_6[14]-4,11-dieneN$_4$)(S_2O_5)]·MeCN (2)

Atom[a]	*x/a*	*y/b*	*z/c*
Fe	0[b]	4618(1)	2500[b]
S(1)	−1029(4)	6458(2)	2749(2)
O(1)	−1009(9)	5613(5)	3084(6)
O(2)	−1999(11)	6565(7)	1975(8)
O(3)	−1146(24)	7015(11)	3366(11)
N(1)	2103(9)	4356(6)	3173(6)
N(2)	763(10)	3853(6)	1518(6)
C(1)	2701(13)	3721(8)	2666(9)
C(2)	2310(13)	3824(8)	1719(8)
C(3)	216(14)	3463(8)	877(8)
C(4)	900(16)	2943(9)	265(10)
C(5)	2289(13)	4215(7)	4134(8)
C(6)	1442(14)	3496(8)	4391(9)
C(7)	1800(16)	4982(9)	4558(9)
C(8)	3811(15)	4076(10)	4464(10)
C(9)	5000[b]	4122(16)	7500[b]
C(10)	5000[b]	3254(14)	7500[b]
N(3)	5000[b]	4761(15)	7500[b]

[a]The numbering scheme for the iron complex is provided in Fig. 5. That for the acetonitrile solvate molecule is N_3-C_9-C_{10}. [b]Fixed parameter; not refined.

Results and Discussion

[(Fe(TPP))$_2$SO$_4$]·C$_6$H$_6$·2SO$_2$

Sulfur dioxide was passed through a benzene solution of Fe(TPP) in an attempted preparation of a substrate-analogue complex of the type Fe(TPP)-(SO_2). Single crystals suitable for X-ray analysis were readily obtained. The subsequent structure determination showed that these crystals contained two Fe^{III}(TPP) units bridged by a sulfate ligand bound in a monodentate mode to each Fe atom. The two halves are related by a C_2 axis containing the sulfur atom of the bridging ligand. While this work was underway, Scheidt *et al.* [17] reported the structure of [(Fe(TPP))$_2$SO$_4$] prepared by an alternative route. The compound was isolated as a chloroform/water solvate in rhombohedral space group $R3m$, where the same C_2 axis is imposed. The present compound crystallizes in orthorhombic space group $P2_122_1$. The unit cell contains two molecules of [(Fe(TPP))$_2$SO$_4$], and two benzene and four sulfur dioxide molecules of solvation. Because of these differences, the structure refinement was pursued. The crystallographically unique part of [(Fe(TPP))$_2$SO$_4$] is shown in Fig. 1, the coordination and bridging units are depicted in Fig. 2 together with bond angles at sulfur, and a stereoview of the entire molecule is available in Fig. 3. Selected metric data are set out in Table 4. The solvate molecules show appreciable thermal motion but are otherwise unexceptional.

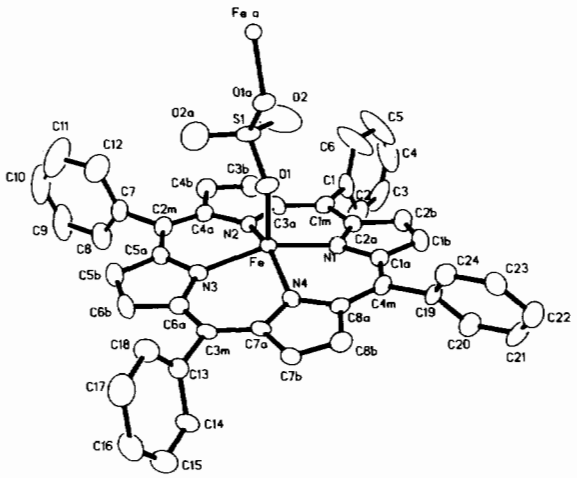

Fig. 1. The crystallographically unique portion of [(Fe(TPP))$_2$SO$_4$], including the atom numbering scheme; atom sizes are scaled to 50% probability ellipsoids.

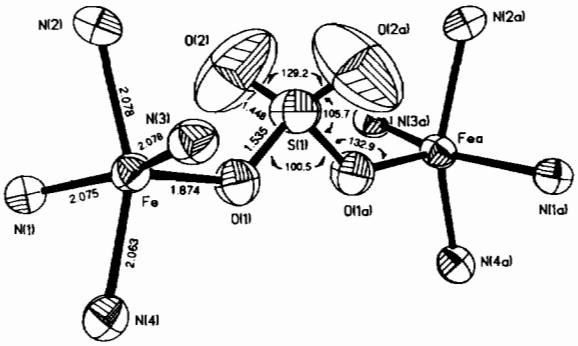

Fig. 2. The coordination units and bridge fragment of [(Fe(TPP))$_2$SO$_4$], including 50% probability ellipsoids and selected bond distances (Å) and angles (°).

The stereochemistry at the Fe atom is entirely typical of five-coordinate, high-spin Fe(III) porphyrin complexes [30]. The Fe atom is displaced 0.47 Å above the N_4 mean plane and 0.49 Å above the mean plane of the porphyrin, at a mean Fe–N distance of 2.074(7) Å. The corresponding values in the rhombohedral form are 0.43 Å and 0.44 Å [17], respectively. As might be expected from the dissimilar packing arrangements, the orthorhombic (O) and rhombohedral (R) forms exhibit small dimensional differences in their porphyrin complexes. The uncoordinated S–O distances (1.43–1.45 Å) are quite comparable, but the coordinated S–O distance is slightly longer in O (1.535(6) Å) than in R (1.512(6) Å). The bridging angle O(1)–S(1)–O(1a) is very close to 101° for both structures, but the angle subtended between the uncoordinated oxygen atoms, O(2)–S(1)–O(2a), is 129.2(7)° for O and 116.5(5)° for R. The Fe–O(1) distance in O (1.874(5) Å) is somewhat shorter than that in R (1.894(4) Å), and the Fe–O(1)–S angle is 3.9° larger in O than in R. The effects

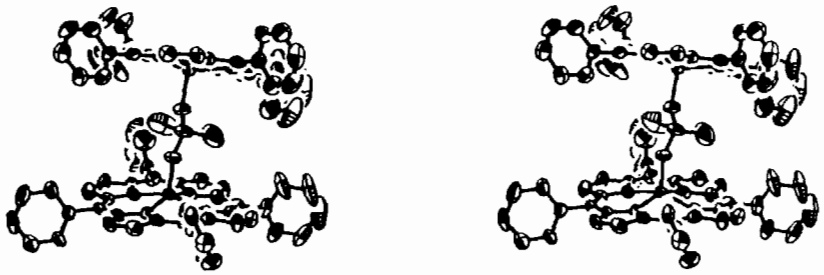

Fig. 3. Stereoview of the structure of $[(Fe(TPP))_2SO_4]$. Atom sizes are scaled to 50% probability ellipsoids.

TABLE 4. Selected Interatomic Distances (Å) and Angles (°) for $[(Fe(TPP))_2SO_4]\cdot C_6H_6\cdot 2SO_2$ [a] (1)

Fe–O(1)	1.874(5)		
S(1)–O(1)	1.535(6)	S(1)–O(2)	1.448(14)
Fe–N(1)	2.075(7)	Fe–N(2)	2.078(6)
Fe–N(3)	2.078(6)	Fe–N(4)	2.063(7)
	Mean Fe–N 2.074(7)[b]		
N(1)–C(a2)	1.368(10)	N(1)–C(a1)	1.397(10)
N(2)–C(a4)	1.385(10)	N(2)–C(a3)	1.369(11)
N(3)–C(a6)	1.394(10)	N(3)–C(a5)	1.349(10)
N(4)–C(a8)	1.374(11)	N(4)–C(a7)	1.385(10)
	Mean $N–C_a$ 1.378(16)		
C(a1)–C(b1)	1.430(12)	C(a2)–C(b2)	1.432(12)
C(a3)–C(b3)	1.421(11)	C(a4)–C(b4)	1.442(8)
C(a5)–C(b5)	1.466(12)	C(a6)–C(b6)	1.434(12)
C(a7)–C(b7)	1.428(12)	C(a8)–C(b8)	1.423(12)
	Mean $C_a–C_b$ 1.435(14)		
C(m1)–C(a3)	1.409(13)	C(m1)–C(a2)	1.407(11)
C(m2)–C(a4)	1.383(13)	C(m2)–C(a5)	1.400(12)
C(m3)–C(a6)	1.379(12)	C(m3)–C(a7)	1.411(12)
C(m4)–C(a1)	1.398(12)	C(m4)–C(a8)	1.408(12)
	Mean $C_m–C_a$ 1.399(12)		
C(b1)–C(b2)	1.340(12)	C(b3)–C(b4)	1.376(14)
C(b5)–C(b6)	1.376(15)	C(b7)–C(b8)	1.370(13)
	Mean $C_b–C_b$ 1.366(17)		
C(m1)–C(1)	1.495(12)	C(m2)–C(7)	1.520(12)
C(m3)–C(13)	1.503(11)	C(m4)–C(19)	1.494(10)
	Mean $C_m–C_\phi$ 1.503(12)		
C(1)–C(2)	1.363(17)	C(1)–C(6)	1.373(19)
C(2)–C(3)	1.412(17)	C(3)–C(4)	1.363(30)
C(4)–C(5)	1.330(34)	C(5)–C(6)	1.394(22)
C(7)–C(8)	1.362(18)	C(7)–C(12)	1.437(21)
C(8)–C(9)	1.433(18)	C(9)–C(10)	1.367(36)
C(10)–C(11)	1.379(39)	C(11)–C(12)	1.398(23)
C(19)–C(20)	1.400(13)	C(19)–C(24)	1.364(12)
C(20)–C(21)	1.392(15)	C(21)–C(22)	1.368(17)
C(22)–C(23)	1.379(15)	C(23)–C(24)	1.386(13)
C(13)–C(14)	1.398(13)	C(13)–C(18)	1.379(15)
C(14)–C(15)	1.390(15)	C(15)–C(16)	1.347(20)
C(16)–C(17)	1.371(20)	C(17)–C(18)	1.414(15)
	Mean $C_\phi–C_\phi$ 1.383(25)		

(continued)

TABLE 4. *(continued)*

O(1)–S–O(1a)	100.5(7)	O(1)–S–O(2)	105.7(7)
O(2)–S–O(1a)	106.1(7)	O(2)–S–O(2a)	129.2(7)
Fe–O(1)–S	132.9(4)		
N(1)–Fe–N(2)	86.9(2)	N(1)–Fe–N(4)	86.9(2)
N(2)–Fe–N(3)	87.2(2)	N(3)–Fe–N(4)	87.4(2)
N(1)–Fe–N(3)	155.0(3)	N(2)–Fe–N(4)	152.9(3)
N(1)–Fe–O(1)	101.5(3)	N(2)–Fe–O(1)	102.9(3)
N(3)–Fe–O(1)	103.5(3)	N(4)–Fe–O(1)	104.2(2)
Fe–N(1)–C(a1)	124.9(5)	Fe–N(1)–C(a2)	127.9(5)
Fe–N(2)–C(a3)	126.2(5)	Fe–N(2)–C(a4)	124.0(5)
Fe–N(3)–C(a5)	124.1(5)	Fe–N(3)–C(a6)	127.5(5)
Fe–N(4)–C(a7)	126.9(5)	Fe–N(4)–C(a8)	125.9(5)
	Mean Fe–N–C_a 125.9(15)		
C(a1)–N(1)–C(a2)	105.3(6)	C(a3)–N(2)–C(a4)	107.0(6)
C(a5)–N(3)–C(a6)	107.2(6)	C(a7)–N(4)–C(a8)	105.7(6)
	Mean C_a–N–C_a 106.3(9)		
N(1)–C(a1)–C(b1)	109.4(7)	N(1)–C(a2)–C(b2)	110.4(7)
N(2)–C(a3)–C(b3)	109.6(8)	N(2)–C(a4)–C(b4)	109.1(7)
N(3)–C(a5)–C(b5)	110.9(8)	N(3)–C(a6)–C(b6)	108.4(7)
N(4)–C(a7)–C(b7)	110.9(7)	N(4)–C(a8)–C(b8)	109.6(7)
	Mean N–C_a–C_b 109.8(9)		
C(a1)–C(b1)–C(b2)	107.6(8)	C(a2)–C(b2)–C(b1)	107.3(8)
C(a3)–C(b3)–C(b4)	107.5(8)	C(a4)–C(b4)–C(b3)	106.7(7)
C(a5)–C(b5)–C(b6)	104.9(9)	C(a6)–C(b6)–C(b5)	108.5(8)
C(a7)–C(b7)–C(b8)	105.4(7)	C(a8)–C(b8)–C(b7)	108.4(7)
	Mean C_a–C_b–C_b 107.0(13)		
C(a2)–C(m1)–C(a3)	123.8(8)	C(a4)–C(m2)–C(a5)	124.3(8)
C(a6)–C(m3)–C(a7)	124.8(7)	C(a1)–C(m4)–C(a8)	124.0(7)
	Mean C_a–C_m–C_a 124.2(4)		
C(a3)–C(m1)–C(1)	118.1(7)	C(a2)–C(m1)–C(1)	118.2(8)
C(a1)–C(m4)–C(19)	120.2(7)	C(a8)–C(m4)–C(19)	115.8(7)
C(a7)–C(m3)–C(13)	117.2(7)	C(a6)–C(m3)–C(13)	118.0(8)
C(a4)–C(m2)–C(7)	116.3(7)	C(a5)–C(m2)–C(7)	119.3(8)
	Mean C_a–C_m–C_ϕ 117.9(14)		
C(6)–C(1)–C(2)	120.8(11)	C(1)–C(2)–C(3)	119.5(14)
C(2)–C(3)–C(4)	120.1(16)	C(3)–C(4)–C(5)	118.3(14)
C(4)–C(5)–C(6)	124.3(19)	C(5)–C(6)–C(1)	116.8(19)
C(24)–C(19)–C(20)	118.2(7)	C(19)–C(20)–C(21)	119.8(9)
C(20)–C(21)–C(22)	121.4(10)	C(21)–C(22)–C(23)	118.5(9)
C(22)–C(23)–C(24)	120.6(9)	C(23)–C(24)–C(19)	121.6(8)
C(18)–C(13)–C(14)	120.4(8)	C(13)–C(14)–C(15)	119.6(10)
C(14)–C(15)–C(16)	121.1(11)	C(15)–C(16)–C(17)	119.5(9)
C(16)–C(17)–C(18)	121.8(12)	C(17)–C(18)–C(13)	117.6(11)
C(12)–C(7)–C(8)	121.9(12)	C(7)–C(8)–C(9)	121.3(18)
C(8)–C(9)–C(10)	116.8(20)	C(9)–C(10)–C(11)	121.8(16)
C(10)–C(11)–C(12)	123.2(26)	C(11)–C(12)–C(7)	114.8(21)
	C(25)–C(26)	1.262(25)	
	C(26)–C(27)	1.287(30)	
	C(27)–C(28)	1.393(32)	
	S(2)–O(3)	1.416(19)	
	S(2)–O(4)	1.317(19)	
	O(3)–S(2)–O(4)	115.5(14)	

[a]The numbering scheme for the porphyrin ring is provided in Fig. 1. [b]In this and Table 5 the standard deviation of the mean is estimated from $\sigma \sim s = [(\Sigma x_i^2 - n\bar{x}^2)/(n-1)]^{1/2}$.

combine to give a greater separation between Fe atoms in O (6.077 Å) than in R (6.049 Å). Finally, the dihedral angles between porphyrin mean planes are 15° (O) and 24° (R), and the rings are rotated so as to reduce interaction among phenyl substituents. The close similarity of the two structures of $[(Fe(TPP))_2SO_4]$ in different lattices suggests that the observed arrangements represent the most stable stereochemistry of the complex.

The formation of $[(Fe(TPP))_2SO_4]$ in the reaction of Fe(TPP) and SO_2 is doubtless due to adventitious dioxygen, despite the care taken to maintain anaerobic conditions. Miksztal and Valentine [31] report spectroscopic evidence for the similar reactions (4) in toluene. Thus, $[(Fe(TPP))_2SO_4]$ is produced when the μ-peroxo dimer $[Fe(TPP)]_2O_2$, formed by exposure of Fe(TPP) to dioxygen at −77 °C, is treated with SO_2 at that temperature; and when a solution of Fe(TPP) saturated with SO_2 is exposed to dioxygen at room temperature. In the latter case, it is concluded that the unstable μ-peroxo complex is trapped by SO_2 prior to dissociation of the O–O bond [31], an established reaction of peroxide-bridged Fe(III) porphyrins [32]. Although the 'sulfato' reaction (5), whereby a sulfate complex is formed by the reverse sequence of events, is well established for a number of metals [11], such a mechanism leading to a μ-SO_4^{2-} complex would require formation of bridge **4** or **5**. There appear to be no examples of **4**, and in **5** the Fe–S–Fe angle would be too small to accommodate opposing porphyrin rings. The largest M–S–M angle reported for **5** is 118° in $[(C_5H_5)Fe(CO)_2]_2SO_2$ [33]. By comparison, the Fe–O–Fe angle in $[Fe(TPP)]_2O$ is 174.5° [34].

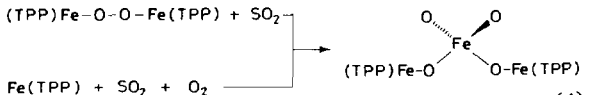

(4)

$$M(SO_2) + O_2 \longrightarrow M(SO_4) \qquad (5)$$

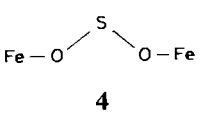

4

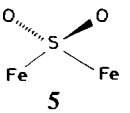

5

[Fe(Me$_6$[14]-4,11-dieneN$_4$)(S$_2$O$_5$)]·MeCN

Reaction (6) in acetonitrile with two equivalents of bisulfite added initially affords the product disulfite complex **2** in reproducible yield. Attempts to improve the yield by further concentrating the reaction mixture were complicated by coprecipitation of $(n\text{-}Bu_4N)CF_3SO_3$. Additional HSO_3^- in the reaction did not improve the yield. The source of $S_2O_5^{2-}$ is presumably the dehydration equilibrium (7), which is well known in aqueous solution. Maylor *et al.* [23] report that R_4N^+ ions with R = Et or a larger group stabilize HSO_3^- relative to $S_2O_5^{2-}$, with the result that the salts $(R_4N)HSO_3$ can be isolated from aqueous solution. The n-Bu_4N^+ salt was used in reaction (6). The equilibrium constant for reaction (7) has the value 0.088 M^{-1} in 1 M $NaClO_4$ solution at 25 °C [35]. This reaction has not been directly established in acetonitrile, but its postulation is reasonable based on the behavior in aqueous solution.

$$[Fe(Me_6[14]\text{-}4,11\text{-}dieneN_4)(MeCN)_2]^{2+} + 2HSO_3^- \longrightarrow [Fe(Me_6[14]\text{-}4,11\text{-}dieneN_4)(S_2O_5)] + H_2O + 2MeCN \qquad (6)$$

$$2HSO_3^- \rightleftharpoons S_2O_5^{2-} + H_2O \qquad (7)$$

[Fe(Me$_6$[14]-4,11-dieneN$_4$)(S$_2$O$_5$)] was obtained as a yellow crystalline compound soluble in Me_2SO and chloroform, and somewhat less soluble in acetonitrile and nitromethane. It is unstable in aqueous solution. The compound is high-spin (5.07 μ_B in chloroform at 23 °C) and exhibits an isotropically shifted ^1H NMR spectrum. The absorption spectrum, shown in Fig. 4, consists of two LMCT bands in the UV region, and two ligand field bands of $^5T_{2g} \rightarrow {}^5E_g$ parentage, at 858 and 1080 nm. No OH stretches were observed in the infrared spectrum, supporting formulation of the ligand as $S_2O_5^{2-}$.

The structure of [Fe(Me$_6$[14]-4,11-dieneN$_4$)(S$_2$O$_5$)] is given in Fig. 5 and a stereoview is provided in Fig. 6. Selected interatomic distances and angles are collected in Table 5. The unit cell contains four Fe complexes and four acetonitrile molecules of

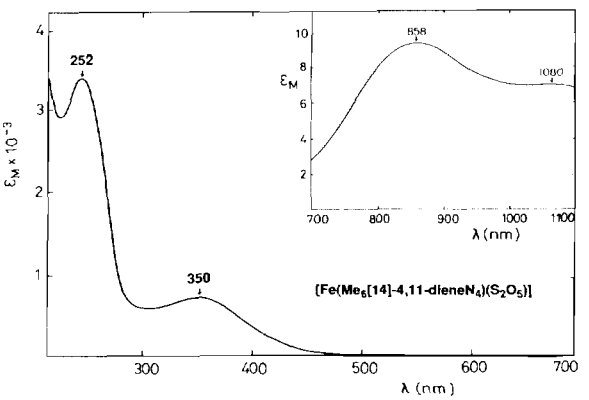

Fig. 4. The UV–Vis spectrum of [Fe(Me$_6$[14]-4,11-dieneN$_4$)(S$_2$O$_5$)] in acetonitrile solution at 22 °C.

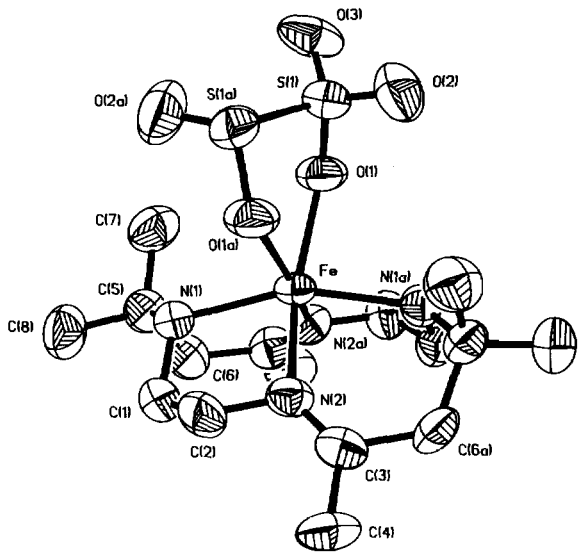

Fig. 5. The structure of [Fe(Me_6[14]-4,11-dieneN$_4$)(S_2O_5)], showing the atom numbering scheme and 50% probability ellipsoids.

solvation. The latter are located on two-fold axes and exhibit a small degree of disorder. Each complex has a two-fold axis running through the Fe atom relating the halves of the macrocycle and of the disulfite ligand. In order for the latter to accommodate this symmetry, the ligand was modelled with an oxygen atom disordered over two sites. Depicted in Fig. 5 is one of two equally weighted structures. The somewhat high *R* value for the structure is a consequence of poor crystal quality. Attempts to grow more suitable crystals were unsuccessful.

[Fe(Me_6[14]-4,11-dieneN$_4$)(S_2O_5)] contains Fe(II) bound to a chelating disulfite and the four nitrogen atoms of the macrocyclic ring. The chelated structure may provide a driving force for reaction (6). The macrocycle is folded down and away from the $S_2O_5^{2-}$ ligand, resulting in strongly distorted octahedral geometry. Consistent with the six-coordinate geometry, this folding is more pronounced than in the case of five-coordinate [Fe-(Me_6[14]-4,11-dieneN$_4$)Cl]$^+$ [36], as evidenced by the smaller angles subtended at iron by nitrogen atoms on opposite sides of the macrocyclic ring. Thus, N(1)–Fe–N(1a) and N(2)–Fe–N(2a) are 156.8(5)° and 109.1(5)°, respectively, for the present structure, while the corresponding values for the five-coordinate complex are 159.9(5)° and 117.7(6)°. The Fe–N distances of 2.162(8) Å and 2.184(10) Å are

TABLE 5. Selected Interatomic Distances (Å) and Angles (°) for [Fe(Me_6[14]-4,11-dieneN$_4$)(S_2O_5)]·MeCN[a] (2)

Fe–O(1)	2.173(9)		
Fe–N(1)	2.162(8)	Fe–N(2)	2.184(10)
S(1)–O(1)	1.490(8)	S(1)–O(2)	1.405(11)
S(1)–O(3)	1.342(19)	S(1)–S(1a)	2.222(7)
N(1)–C(1)	1.476(16)	N(1)–C(5)	1.482(15)
N(2)–C(2)	1.466(15)	N(2)–C(3)	1.228(15)
C(1)–C(2)	1.459(18)	C(3)–C(4)	1.500(21)
C(3)–C(6a)	1.579(19)	C(5)–C(6)	1.527(18)
C(5)–C(7)	1.534(20)	C(5)–C(8)	1.486(18)
N(3)–C(9)	1.058(37)	C(9)–C(10)	1.437(36)
Fe–O(1)–S(1)	123.4(6)	O(1)–Fe–O(1a)	81.4(5)
O(1)–S(1)–O(2)	112.6(6)	O(1)–S(1)–O(3)	113.5(9)
O(1)–S(1)–S(1a)	98.9(4)	O(2)–S(1)–O(3)	113.5(10)
S(1a)–S(1)–O(2)	102.3(5)	S(1a)–S(1)–O(3)	114.8(10)
N(1)–Fe–O(1)	113.2(3)	N(1)–Fe–O(1a)	84.9(3)
N(2)–Fe–O(1)	160.7(3)	N(2)–Fe–O(1a)	86.3(3)
N(1)–Fe–N(2)	80.2(3)	N(1)–Fe–N(2a)	86.4(4)
N(1)–Fe–N(1a)	156.8(5)	N(2)–Fe–N(2a)	109.1(5)
Fe–N(1)–C(1)	107.4(6)	N(1)–C(1)–C(2)	112.6(10)
Fe–N(2)–C(2)	107.9(7)	N(2)–C(2)–C(1)	108.1(11)
Fe–N(1)–C(5)	118.1(7)	C(1)–N(1)–C(5)	114.8(9)
N(1)–C(5)–C(6)	113.3(9)	N(1)–C(5)–C(7)	107.4(10)
N(1)–C(5)–C(8)	109.1(11)	C(7)–C(5)–C(8)	109.2(11)
C(6)–C(5)–C(7)	109.0(11)	C(5)–C(6)–C(3a)	120.8(10)
Fe–N(2)–C(3)	135.7(9)	C(2)–N(2)–C(3)	116.4(11)
N(2)–C(3)–C(6a)	118.7(12)	N(2)–C(3)–C(4)	129.4(13)
C(4)–C(3)–C(6a)	111.9(10)		

[a]The numbering scheme for the iron complex is provided in Fig. 5. That for the acetonitrile solvate molecule is N_3-C_9-C_{10}.

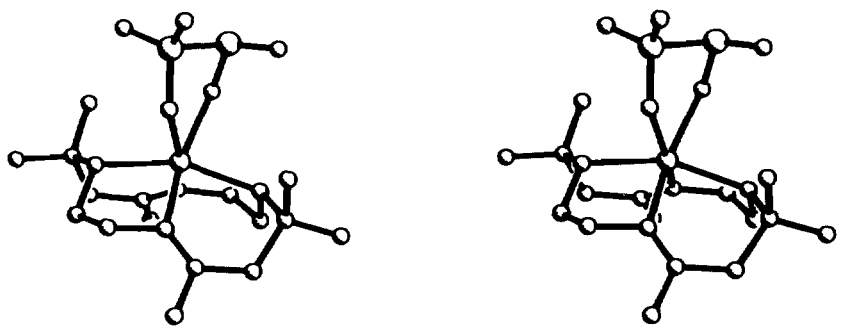

Fig. 6. Stereoview of the structure of [Fe(Me_6[14]-4,11-dieneN$_4$)(S_2O_5)].

typical for high-spin Fe^{II}–N bonds [37]*. The dihedral angle between the (Fe,O1,O1a) and (Fe,N2, N2a) mean planes is 18.3°. The structures of complexes of the Curtis and related tetraaza macrocycles have been summarized [38].

The S–S bond length in the disulfite ligand is 2.222(7) Å, a value indistinguishable from 2.2194(9) Å in the free anion as its potassium salt [39]. The coordinated S–O bonds are, as expected, somewhat longer than the 1.45–1.47 Å distances in free $S_2O_5^{2-}$, while the bonds from sulfur to uncoordinated oxygen are shorter (1.405(11), 1.342(19) Å). The O(1)–S(1)–S(1a) angle in the coordinated ligand (98.9(4)°) is virtually unchanged from that of the free species (99.12(3)°). The Fe–O(1) distance of 2.173(9) Å is consistent with the range (2.04–2.17 Å) of Fe–O bond lengths observed for sulfite ion coordinated to Fe(II) in several hydrated forms of $FeSO_3$ [40, 41]. The structural evidence clearly shows practically no distortion of the structure of disulfite when acting as a chelate ligand to Fe(II).

The precursor complex *trans*-$[Fe(Me_6[14]\text{-}4,11\text{-}dieneN_4)(MeCN)_2]^{2+}$ contains low-spin Fe(II) [42] as a result of the ligand field strength of the N_6 coordination unit. The Fe(II) ionic radius of the low-spin state is small enough to allow the metal to reside in the N_4 plane of the macrocycle. In the presence of the weaker field oxygen ligands supplied by disulfite, Fe(II) is high-spin and can no longer be accommodated in the N_4 plane. In the case of weak-field halide ligands, the complexes $[Fe(Me_6\text{-}[14]\text{-}4,11\text{-}dieneN_4)X]^+$ are high-spin and the coordination number is limited to five [38, 43]. Dimerization of bisulfite to yield a bidentate ligand suitable to the geometric constraints of the macrocyclic complex permits additional stabilization of six-coordinate, high-spin Fe(II).

As noted at the outset, this work provides the first structurally characterized example of a transition metal disulfite complex**. With reference to pathways (2) and (3), it is evident that if SO_2 complexes of Fe(II) porphyrins are to be obtained, even more rigorously anaerobic conditions than those employed here must be applied. Further, coordination of bisulfite or sulfite to a Fe(II) tetraaza macrocycle will require suppression of equilibrium (7) in favor of the desired ligand and/or the use of five-coordinate complexes such that monodentate binding will be promoted. The recent electrochemical production of H_2S mediated by a water-soluble iron porphyrin in an aqueous system to which bisulfite had been added [45] renders even more attractive the investigation of pathways such as (2) and (3) in order to model the substrate complex and identify intermediates in reaction (1), one of only three six-electron reductions in biology.

*Low-spin Fe(II)–N bonds are typically *ca.* 1.97 Å in length.

**Infrared spectroscopic and analytical data have been reported for a material formulated as $Cu_2S_2O_5$ [44]. The structure of this compound has not been reported.

Supplementary Material

Anisotropic temperature factors for non-hydrogen atoms and structure factor tables are available from the authors on request.

Acknowledgements

This research was supported by NIH Grant GM 28856. X-ray diffraction equipment was obtained by NIH Grant 1 S10 RR 02247. We thank Dr Ch. Pulla Rao and Derk Wierda for assistance with the crystallography.

References

1 J. W. Anderson, *Sulfur in Biology*, University Park Press, Baltimore, 1978.
2 J. R. Postgate, in G. Nickless (ed.), *Inorganic Sulfur Chemistry*, Elsevier, New York, 1968, Ch. 8.
3 L. M. Siegel, D. C. Rueger, M. J. Barber, R. J. Krueger, N. R. Orme-Johnson and W. H. Orme-Johnson, *J. Biol. Chem., 257* (1982) 6343.
4 (a) P. A. Janick and L. M. Siegel, *Biochemistry, 21* (1982) 3538; (b) J. A. Christner, E. Münck, T. A. Kent, P. A. Janick, J. C. Salerno and L. M. Siegel, *J. Am. Chem. Soc., 106* (1984) 6786; (c) J. F. Cline, P. A. Janick, L. M. Siegel and B. M. Hoffman, *Biochemistry, 24* (1985) 7942.
5 D. E. McRee, D. C. Richardson, J. S. Richardson and L. M. Siegel, *J. Biol. Chem., 261* (1986) 10277.
6 L. H. Vogt, Jr., L. Katz and S. E. Wiberley, *Inorg. Chem., 4* (1965) 1157.
7 (a) K. Gleu, W. Breuel and K. Rehm, *Z. Anorg. Allg. Chem., 235* (1938) 201; (b) K. Gleu and W. Breuel, *Z. Anorg. Allg. Chem., 235* (1938) 211.
8 A. Passoja and L. Lajunen, *Finn. Chem. Lett., 119,* 122 (1980).
9 S. Jagner, E. Ljungström and A. Tullberg, *Acta Crystallogr., Sect. B, 36* (1980) 2213.
10 C. R. Jablonski, *J. Organomet. Chem., 142* (1977) C25.
11 R. R. Ryan, G. J. Kubas, D. C. Moody and P. G. Eller, *Struct. Bonding (Berlin), 46* (1981) 47.
12 W. A. Schenck, J. Leissner and C. Burschka, *Angew. Chem., Int. Ed. Engl., 23* (1984) 806.
13 K. S. Arulsamy, K. K. Pandey and U. C. Agarwala, *Inorg. Chim. Acta, 54* (1981) L51.
14 D. R. English, D. N. Hendrickson, K. S. Suslick, C. W. Eigenbrot, Jr. and W. R. Scheidt, *J. Am. Chem. Soc., 106* (1984) 7258.
15 C. G. Kuehn and H. Taube, *J. Am. Chem. Soc., 98* (1976) 689.
16 M. A. Phillippi, N. Baenziger and H. M. Goff, *Inorg. Chem., 20* (1981) 3904.

17 W. R. Scheidt, Y. J. Lee, T. Bartzcak and K. Hatano, *Inorg. Chem., 23* (1984) 2552.
18 A. D. Adler, F. R. Longo, J. D. Finarelli, J. Goldmacher, J. Assour and L. J. Korsakoff, *J. Org. Chem., 32* (1967) 476.
19 H. Kobayashi, T. Higuchi, Y. Kaizu, H. Osada and M. Aoki, *Bull. Chem. Soc. Jpn., 48* (1975) 3137.
20 A. D. Adler, F. R. Longo and V. Varadi, *Inorg. Synth., 16* (1976) 213.
21 A. M. Stolzenberg, S. H. Strauss and R. H. Holm, *J. Am. Chem. Soc., 103* (1981) 4763.
22 A. M. Tait and D. H. Busch, *Inorg. Synth., 18* (1978) 2.
23 R. Maylor, J. B. Gill and D. C. Goodall, *J. Chem. Soc., Dalton Trans.*, 2001 (1972).
24 D. T. Cromer and J. T. Waber, *International Tables for X-Ray Crystallography*, Kynoch Press, Birmingham, U.K., 1974.
25 R. E. Marsh, *Acta Crystallogr., Sect. B, 42* (1986) 193.
26 D. F. Evans, *J. Chem. Soc.*, (1959) 2003.
27 D. H. Live and S. I. Chan, *Anal. Chem., 42* (1970) 791.
28 *Handbook of Chemistry and Physics*, CRC Press, Boca Raton, FL, 1986, pp. E-124–132.
29 C. J. O'Connor, *Prog. Inorg. Chem., 29* (1982) 203.
30 W. R. Scheidt and C. A. Reed, *Chem. Rev., 81* (1981) 543.
31 A. R. Miksztal and J. S. Valentine, *Inorg. Chem., 23* (1984) 3548.
32 (a) D.-H. Chin, G. N. La Mar and A. L. Balch, *J. Am. Chem. Soc., 102* (1980) 4344, 5947; (b) A. L. Balch, Y.-W. Chan, R.-J. Cheng, G. N. La Mar, L. Latos-Grazynski and M. W. Renner, *J. Am. Chem. Soc., 106* (1984) 7779.
33 M. R. Churchill, B. G. DeBoer and K. Kalra, *Inorg. Chem., 12* (1973) 1646.
34 A. B. Hoffman, D. M. Collins, V. W. Day, E. B. Fleischer, T. S. Srivastava and J. L. Hoard, *J. Am. Chem. Soc., 94* (1972) 3620.
35 R. E. Connick, T. M. Tam and E. von Deuster, *Inorg. Chem., 21* (1982) 103.
36 V. L. Goedken, J. Molin-Case and G. G. Christoph, *Inorg. Chem., 12* (1973) 2894.
37 J. L. Hoard, *Science, 174* (1971) 1295.
38 N. F. Curtis, in G. A. Melson (Ed.), *Coordination Chemistry of Macrocyclic Compounds*, Plenum, New York, 1979, Ch. 4.
39 I.-C. Chen and Y. Wang, *Acta Crystallogr., Sect. C, 40,* (1984) 1780.
40 L.-G. Johansson and O. Lindqvist, *Acta Crystallogr., Sect. B, 35,* (1979) 1017.
41 L.-G. Johansson and E. Ljungström, *Acta Crystallogr., Sect. B, 35* (1979) 2683; *36* (1980) 1184.
42 V. L. Goedken, P. H. Merrell and D. H. Busch, *J. Am. Chem. Soc., 94* (1972) 3397.
43 F. L. Urbach, in G. A. Melson (Ed.), *Coordination Chemistry of Macrocyclic Compounds*, Plenum, New York, 1979, Ch. 5.
44 W. D. Harrison, J. B. Gill and D. C. Goodall, *Polyhedron, 2* (1983) 153.
45 M. A. Kline, M. H. Barley and T. J. Meyer, *Inorg. Chem., 26* (1987) 2197.